EXHIBIT 189

Biochemical and Biophysical Research Communications 653 (2023) 93–101

Contents lists available at ScienceDirect

Biochemical and Biophysical Research Communications

journal homepage: www.elsevier.com/locate/ybbrc

Filamin A is overexpressed in non-alcoholic steatohepatitis and contributes to the progression of inflammation and fibrosis

Ying Lu [a, 1], Mengzhu Wang [b, 1], Manyu Zhao [b], Qianru Zhang [a, b], Rui Qian [b], Zan Hu [a], Qi Ke [c], Lin Yu [d], Liqun Wang [b], Qinhuai Lai [a], Zhenmi Liu [b], Xia Jiang [b], Ben Zhang [b], Jinliang Yang [a, **], Yuqin Yao [a, b, *]

[a] State Key Laboratory of Biotherapy and Cancer Center, West China Hospital, West China School of Public Health and West China Fourth Hospital, Sichuan University, Chengdu, 610041, China
[b] Molecular Toxicology Laboratory of Sichuan Provincial Education Office, Institute of Systems Epidemiology, West China School of Public Health and West China Fourth Hospital, Sichuan University, Chengdu, 610041, China
[c] Department of Pathology, Mianyang Central Hospital, School of Medicine, University of Electronic Science and Technology of China, Mianyang, 621000, China
[d] Department of Clinical Laboratory, Mianyang Central Hospital, School of Medicine, University of Electronic Science and Technology of China, Mianyang, 621000, China

ARTICLE INFO

Article history:
Received 8 February 2023
Received in revised form
15 February 2023
Accepted 18 February 2023
Available online 22 February 2023

Keywords:
Non-alcoholic steatohepatitis
Filamin A
Macrophage
Hepatic stellate cell

ABSTRACT

Non-alcoholic steatohepatitis (NASH) is a chronic and progressive liver disease characterized by steatosis, inflammation, and fibrosis. Filamin A (FLNA), an actin-binding protein, is involved in various cell functions, including the regulation of immune cells and fibroblasts. However, its role in the development of NASH through inflammation and fibrogenesis is not fully understood. In this study, we found that FLNA expression was increased in liver tissues of patients with cirrhosis and mice with non-alcoholic fatty liver disease (NAFLD)/NASH and fibrosis. Immunofluorescence analysis showed that FLNA was primarily expressed in macrophages and hepatic stellate cells (HSCs). Knocking down of FLNA by specific shRNA in phorbol-12-myristate-13-acetate (PMA)-derived THP-1 macrophages reduced lipopolysaccharide (LPS)-stimulated inflammatory response. The decreased mRNA levels of inflammatory cytokines and chemokines and suppression of the STAT3 signaling were observed in FLNA-downregulated macrophages. In addition, knockdown of FLNA in immortalized human hepatic stellate cells (LX-2 cells) resulted in decreased mRNA levels of fibrotic cytokines and enzymes involved in collagen synthesis, as well as increased levels of metalloproteinases and pro-apoptotic proteins. Overall, these results suggest that FLNA may contribute to the pathogenesis of NASH through its role in the regulation of inflammatory and fibrotic mediators.

1. Introduction

NAFLD is a rapidly growing health concern that affects up to 25% of the global population [1]. NASH, an advanced form of NAFLD, increases the risk of developing cirrhosis and hepatocellular carcinoma [2]. The pathophysiology of NASH is complex and multifactorial. Hepatic inflammation, which is caused by a variety of molecular mechanisms such as lipotoxicity, molecules associated with hepatocyte damage, and gut-derived endotoxins, plays a key role in the progression of NASH.

Activation of liver innate immune system has been found to contribute to liver damage in NASH [3]. Macrophages, which are a type of immune cell, play a critical role in NASH [4]. When activated, liver resident macrophages (called Kupffer cells) release chemokines that recruit monocytes to the liver. These monocyte-

* Corresponding author. Molecular Toxicology Laboratory of Sichuan Provincial Education office, Institute of Systems Epidemiology, West China School of Public Health and West China Fourth Hospital, Sichuan University, Chengdu, Sichuan, 610041, China.
** Corresponding author. State Key Laboratory of Biotherapy and Cancer Center, West China Hospital, Sichuan University, Chengdu, Sichuan, 610041, China.
E-mail addresses: jinliangyang@scu.edu.cn (J. Yang), yuqin_yao@scu.edu.cn (Y. Yao).
[1] The first two authors contributed equally to this work.

https://doi.org/10.1016/j.bbrc.2023.02.048

derived macrophages further amplify liver injury by producing pro-inflammatory cytokines and reactive oxygen species. Macrophages can also attract neutrophils and lymphocytes, stimulate HSCs to transform into collagen-producing myofibroblasts, and promote the formation of new blood vessels and scar tissue [5]. Therefore, understanding the mechanisms behind macrophage function may provide new insights and strategies for NASH.

FLNA is a cytoskeletal actin-binding protein that helps organize actin filaments and connect them to cell membranes [6]. It has been found to be involved in various cell functions such as signal transduction, proliferation, differentiation, and migration [7]. Its deficiency in T cells affects their ability to traffic to the site of inflammation [8]. FLNA has been implicated in the migration and phagocytosis in human neutrophil-like HL-60 cells [9], and the development of aortic plaque in atherosclerosis [10]. FLNA also promotes fibroblast proliferation and regulates the remodeling of pericellular collagen matrix in fibroblasts [11], and contributes to the differentiation of cardiac fibroblasts into myofibroblasts in inflammation-mediated myocardial fibrosis [12]. In this study, we observed increased expression of FLNA in the livers of patients with cirrhosis and mice with NAFLD/NASH and fibrosis. Based on these observations, we hypothesized that FLNA may be involved in the development of NASH. Hence, we used shRNA-mediated knockdown to decrease FLNA expression in macrophages and HSCs in vitro and analyzed the effects on gene expression. These results suggested that FLNA may contribute to the pathogenesis of NASH through its role in the regulation of inflammatory and fibrotic mediators in these cell types.

2. Materials and methods

2.1. Animal studies

Male 6-week-old C57BL/6J mice were purchased from the Vital River Laboratory Animal Technology Co., Ltd. (Beijing, China). Mice were maintained in a specific pathogen-free facility under 12/12-hr light/dark cycles with free access to food and water. All animal studies were performed following the standard guidelines and were approved by the institutional animal care and treatment committee of West China Hospital, Sichuan University (2019273A). Mice were fed with NAFLD/NASH diets at nine weeks of age. For a period of 8 weeks, a group of 10 mice were fed a methionine- and choline-deficient diet (MCD) (TP-3005G, Trophic Animal Feed High-Tech Co., Ltd, Nantong, China). Another group of 10 mice were given a choline-deficient, L-amino acid-defined high-fat diet (CDAHFD) (A06071302, Research Diets Inc) for 12 weeks. A group of 8 mice were provided with an amylin diet (AMLN) (D09100301, Research Diets Inc) high in *trans*-fats, cholesterol, and fructose for 41 weeks. Additionally, a group of 10 mice were given a high-fat diet (HFD) (D12492, Research Diets Inc) for 36 weeks. In the control groups, mice were fed normal chow (DASHOU, Chengdu, China) for the corresponding weeks of the different diets. There were 8 mice that served as controls for the AMLN diet, and 5 mice each that served as controls for the MCD, CDAHFD, and HFD diets. To induce acute liver fibrosis, 9-week-old mice were intraperitoneally injected with vehicle (N = 3) or 25% carbon tetrachloride (CCl_4) (Sigma, 319961) (N = 6) dissolved in olive oil at 2 mL/kg twice a week for six weeks. Upon completion of the feeding regimen, animals were anesthetized with pentobarbital sodium and sacrificed. Blood and liver tissues were collected and stored for further analysis.

2.2. Liver histology and serum chemistry

Fresh mouse liver tissues were fixed in 10% neutral buffered formalin and then embedded in paraffin. The formalin-fixed paraffin-embedded slides of healthy human liver were purchased from Shanghai Outdo Biotech Co., Ltd. (Shanghai, China). The formalin-fixed paraffin-embedded slides of cirrhotic human liver were obtained from Mianyang Central Hospital. Paraffin sections were stained with hematoxylin and eosin (H&E) for histomorphometric analysis. Sirius red staining was performed to evaluate liver fibrosis. The degree of steatosis, inflammation, and ballooning was assessed by two experienced pathologists in a blinded manner using the NAFLD activity score (NAS) system [13]. Liver tissues were also subjected to immunohistochemistry and immunofluorescence to analyze FLNA expression and the localization of cells. The antibodies against FLNA (Huabio, ET1601-3), α-smooth muscle actin (α-SMA) (Huabio, ET1607-53), and F4/80 (Abcam, ab6640) were used. All the stained slices were scanned using a Pannoramic scanner (3DHISTECH, Budapest, Hungary).

Serum concentrations of alanine aminotransferase (ALT), aspartate aminotransferase (AST), alkaline phosphatase (ALP), total cholesterol (TC), low-density lipoprotein (LDL), and high-density lipoprotein (HDL) were measured using the chemistry analyzer (Hitachi 7020, Tokyo, Japan) following the manufacturer's instructions.

2.3. Cell culture and treatment

The human monocytic cell line (THP-1) and mouse RAW264.7 macrophage were procured from the American Type Culture Collection (ATCC, USA). The immortalized human Hepatic stellate cell line (LX-2) was obtained from Procell Life Science & Technology Co., Ltd. Rat HSCs were isolated from Sprague-Dawley rat livers by two-step perfusion and Nycodenz density gradient centrifugation [14]. THP-1 and RAW264.7 cells were grown in RPMI-1640 with 10% fetal bovine serum (FBS). LX-2 and rat HSC were grown in DMEM medium with 20% FBS. The culture medium was supplemented with penicillin/streptomycin (100 units/mL, 100 μg/mL) (Gibco, USA). To differentiate THP-1 monocytes into macrophage-like structures, the cells were incubated with 50 nM PMA for 48 hours (h) in complete RPMI medium. The cells were then incubated with fresh medium for an additional 24 h and stimulated with LPS (Sigma, L2630) at a concentration of 100 ng/mL for 6 h. The cells were then collected for subsequent experiments.

2.4. RNA-mediated interference

For FLNA silencing, lentiviruses were produced using the vectors consisting of psPAX2, pMD2.G, and expression plasmids pLKO.1-GFP-Puro. The shRNA target sequences (MISSION shRNA clones, Sigma-Aldrich) were shFLNA-1 5′-CGGCACTTTCGACATCTTCTA-3' (TRCN0000062530), shFLNA-2 5′-GACCGCCAATAACGACAAGAA-3' (TRCN0000062532), shFLNA-3 5′-CATGCGTATGTCCCACCTAAA-3' (TRCN0000062531). The empty pLKO.1 vector was used as a control. HEK293T cells were transfected with vectors by jetPRIME® regent (Polyplus, France) to produce lentivirus particles. The medium containing lentiviral particles were harvested 48 h after transfection. The cells in medium were removed by passing through a 0.45 μm filter. For lentivirus infection, the virus-containing medium was added to THP-1 cells that had been pre-seeded in 24-well plates at a density of 80 000 cells per well, in the presence of 8 μg/mL polybrene. 2×10^5 LX-2 cells were infected in 6-well plates with 8 μg/mL polybrene. The virus-containing medium was replaced with fresh medium 24 h after the infection process. After an additional 24 h of incubation, puromycin was added at a concentration of 0.8 μg/mL to select and purify the resistant clones.

To knock down FLNA in mouse RAW264.7 macrophage cells, short interfering RNA (siRNA) and scrambled sequences were

designed and synthesized by General Biosystems Co., Ltd. (Anhui, China). The target sequences for FLNA siRNA were 5′-GCAGCUGCUCAGUAGAAUATT-3′,5′-GGGUCCAUCUAAAGCAGAATT-3′,5′-CCUCAUCUCCAUCAAGUAUTT-3′, and the scramble sequences was 5′-UUCUCCGAACGUGUCACGUTT-3′. RAW264.7 cells were plated in 6-well plates at a density of 2×10^5 cells per well. 50 nM siFLNA and scrambled siRNA were transfected into the cells using lipofectamine 2000 transfection reagent (ThermoFisher, USA) according to the manufacturer's instructions. The transfection medium was changed 12 h after transfection. 48 h post-transfection, cells were exposed to 100 ng/mL LPS for another 6 h. Finally, cells and supernatant were collected for subsequent analysis.

2.5. Transcriptome sequencing and data analysis

The PMA-derived THP-1 macrophages expressing shRNA or shFLNA were treated with LPS and then subjected to transcriptome sequencing. The RNA collection, library preparation, sequencing, and data processing were carried out by Novogene Bioinformatics Technology Co., Ltd. (Beijing, China), as previously described [15]. Differential expression analysis between the two groups was performed using the DESeq2 R package (1.16.1). Genes with an adjusted *p*-value <0.05 were considered differentially expressed. The Cluster Profiler R package was used for the Kyoto Encyclopedia of Genes and Genomes (KEGG) pathway enrichment analysis of the differentially expressed genes (DEGs).

2.6. Quantitative real-time PCR analysis

Total RNAs were extracted from cells or tissues using the RNA isolation kit (Foregene, China). The reverse transcription was performed by HiScript® II Reverse Transcriptase (Vazyme, China) on 1 μg of total RNA template. mRNA levels were then quantified with SYBR Green master mix (Vazyme, China) on a CFX96 real-time PCR system (Bio-Rad, USA) with primers specific for the target gene (Table S1). The levels of the target gene were normalized to β-actin and the relative mRNA fold changes were calculated using the $2^{-\Delta\Delta CT}$ method.

2.7. Western blot

Protein samples were prepared from liver homogenates or cells with RIPA lysis buffer (Beyotime, Shanghai, China) on ice, and protein concentrations were determined using the BCA Protein Assay Kit (Beyotime, Shanghai, China). The protein samples were separated in the 10% SDS-PAGE gel and transferred onto PVDF. The membranes were then blocked with 5% non-fat milk for 1.5 h and incubated overnight at 4 °C with the primary antibodies at a dilution of 1:500–1:1000. The antibodies against Filamin A (ET1601-3), phospho-STAT3 (Tyr705) (ET1603-40), STAT3 (ET1605-45), phospho-STAT1(Ser727) (ET1611-20), STAT1(ET1612-22), phospho-STAT5 (Y694) (ET1610-48) and β-Actin (HA601082) were obtained from Huabio (China). GAPDH antibody (200306-7E4) was obtained from ZenBio (Chengdu, China). Phospho-NF-κB p65 (Ser536) (#3033) and NF-κB p65 (#8242) antibodies were acquired from Cell Signaling Technology (USA). After washing with TBST, the membranes were incubated with horseradish peroxidase-conjugated secondary antibodies at a dilution of 1:5000 for 1 h at room temperature. The proteins were visualized by enhanced chemiluminescence reagents (EpiZyme, USA) in the iBright CL1500 and FL1500 Imaging Systems (ThermoFisher, Singapore).

2.8. ELISA

The concentration of CXCL10 in the culture medium of RAW264.7 cells with indicated treatment was measured by ELISA assay. The mouse CXCL10 ELISA kit was obtained from Neo-Bioscience Technology Co., Ltd (Shenzhen, China). The assay was performed according to the manufacturer's protocol. The absorbance was recorded by a Multiskan GO microplate reader (ThermoFisher, USA).

2.9. Statistical analysis

The data were presented as the mean ± standard error of mean (SEM). SPSS 26.0 was used for statistical analysis. Student's test or Mann-Whitney *U* test was used to compare the differences between two groups, and ANOVA (with Dunnett's or Tukey's post-hoc test for multiple comparison) or Kruskal-Wallis test (Steel Dwass post-hoc test for multiple comparison) was used to compare three or more groups. Correlation analysis was performed using Pearson product moment coefficient. P value < 0.05 was statistically significant.

3. Results

3.1. FLNA was upregulated in experimental liver steatohepatitis and fibrosis

To explore the role of FLNA in the progression of liver steatohepatitis and fibrosis, we developed five different murine models. The pathological signs were characterized as shown in Fig. S1. Then, we evaluated the expression of FLNA in these mice. As determined by immunohistochemistry and immunoblot, FLNA expression was significantly increased in the livers of mice with MCD, CDAHFD, AMLN, and CCl_4, and slightly increased in the HFD liver, which had the least inflammatory cell infiltration and fibrosis formation (Fig. 1A–C). The upregulated hepatic FLNA was also observed at mRNA levels (Fig. 1D). FLNA protein levels were found to be associated with its mRNA levels in the livers of mice with steatohepatitis and fibrosis ($r = 0.6938$, $p < 0.0001$) (Fig. 1E). We also observed higher expression of FLNA in the liver tissues of patients with cirrhosis compared to normal controls (Fig. 1F). Additionally, immunofluorescence analysis showed that FLNA co-located with the macrophage marker F4/80 (Fig. 1G) and the HSC marker α-SMA (Fig. 1H) in CDAHFD-induced NASH liver segments. Overall, liver steatohepatitis and fibrosis were associated with the hepatic upregulation of FLNA expression.

3.2. FLNA knockdown reduced inflammatory factors production in macrophages

To dissect the biological function of FLNA in macrophages, we employed lentivirus-mediated shRNA knockdown to reduce FLNA expression in THP-1 cells with the most effective shFLNA-1 (Fig. S2A). The decrease in FLNA protein levels was verified (Fig. S2B). Quantitative transcriptome analysis provided deep insight into the molecular changes in PMA-derived THP-1 macrophages with or without FLNA knockdown. Compared to the shNC group, there were 307 upregulated genes and 301 downregulated genes in the shFLNA group with a threshold of p value < 0.05 (Fig. 2A). Importantly, these differences were exaggerated in response to LPS stimulation (Fig. 2B). KEGG analysis of the downregulated DEGs showed an accumulation in the Cytokine-cytokine receptor interaction, NOD-like receptor signaling, and JAK-STAT signaling pathways (Fig. 2C). Reactome analysis revealed significant enrichment in signaling by interleukins and interferon signaling (Fig. 2D). qRT-PCR analysis showed the expression of inflammatory cytokines (IL-6, TNF-α, IFNL1, IFNL2), and chemokine ligands (CXCL9, CXCL10, CCL2, CCL3, CCL8) were downregulated in

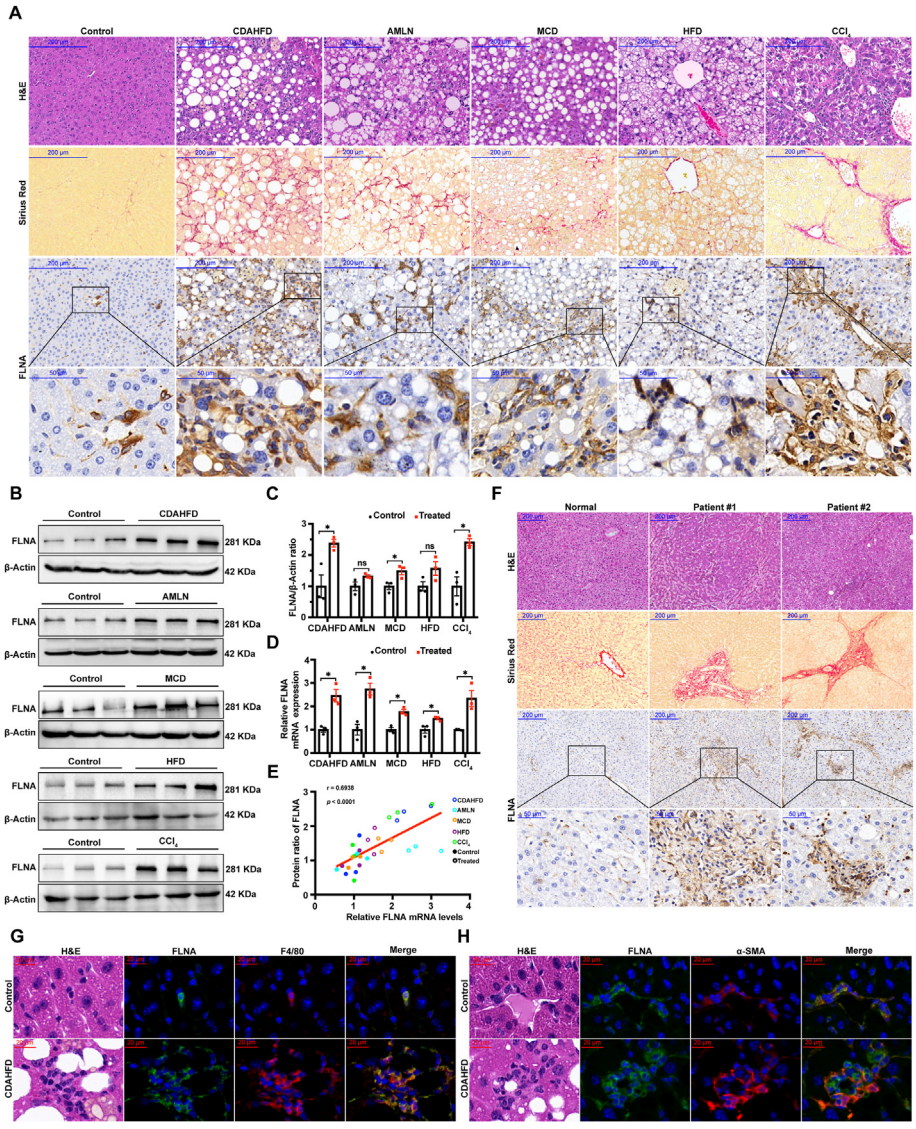

Fig. 1. FLNA expression in hepatic steatohepatitis and fibrosis models. (A) Representative pathological sections of liver tissues from the experimental hepatic steatohepatitis and fibrosis models, including H&E staining (10 ×, scale bar 200 μm), Sirius Red staining (10 ×, scale bar 200 μm), and FLNA immunohistochemical staining (10 ×, scale bar 200 μm; 40 ×, scale bar 50 μm). (B) Western blot analysis of protein levels of FLNA in liver tissues of five different models. (C) Quantification of (B). (D) FLNA mRNA levels of the five models detected by qRT-PCR. (E) Correlation between protein and mRNA levels of FLNA in the five models. (F) Representative pathological sections of liver tissues from healthy controls and patients with cirrhosis, including H&E staining (10 ×, scale bar 200 μm), Sirius Red staining (10 ×, scale bar 200 μm), and FLNA immunohistochemical staining (10 ×, scale bar 200 μm; 40 ×, scale bar 50 μm). (G) The co-localization of FLNA with F4/80 (70 ×, scale bar 20 μm). (H) The co-localization of FLNA with α-SMA (70 ×, scale bar 20 μm). Data are mean ± SEM; $n = 3$. Ns: not significant, $^{*}p < 0.05$, $^{**}p < 0.01$, $^{***}p < 0.001$. (For interpretation of the references to colour in this figure legend, the reader is referred to the Web version of this article.)

the FLNA knockdown macrophages with LPS stimulation (Fig. 2E-N). In addition, the results showed a positive correlation between FLNA mRNA levels and CXCL10 mRNA levels (r = 0.5298, p = 0.0026) in the liver steatohepatitis and fibrosis models (Fig. 2O). A decrease in CXCL10 secretion was observed in FLNA knockdown RAW264.7 cells (Fig. 2P). Consequently, these data indicated that FLNA knockdown reduced the production of inflammatory factors in macrophages upon LPS stimulation.

3.3. FLNA regulated macrophage inflammatory response through STAT3 signaling pathway

Several signaling pathways have been shown to contribute to the inflammatory process of macrophages, including NF-κB, JAK/STAT, and NLRP3 inflammasome activation. Our data showed LPS-stimulated STAT3 phosphorylation at Y705 was suppressed by FLNA knockdown in PMA-derived THP-1 macrophages and RAW264.7 cells. (Fig. 3). However, the phosphorylation levels of several mediators in STAT1/5 (Figs. S2D–F) and NF-κB (Fig. S2G) pathways were slightly or not influenced. These data supported that FLNA facilitated macrophage inflammation by STAT3 signaling.

3.4. FLNA was related to HSCs activation, apoptosis, and profibrotic mediator expression

Activation of the HSCs is the primary source of myofibroblasts, which are responsible for extracellular matrix (ECM) production in the fibrotic liver. Quiescent HSCs were isolated from rat liver and activated by in vitro culture (Fig. 4A). As data shown, the mRNA levels of FLNA increased during the activation of quiescent HSCs

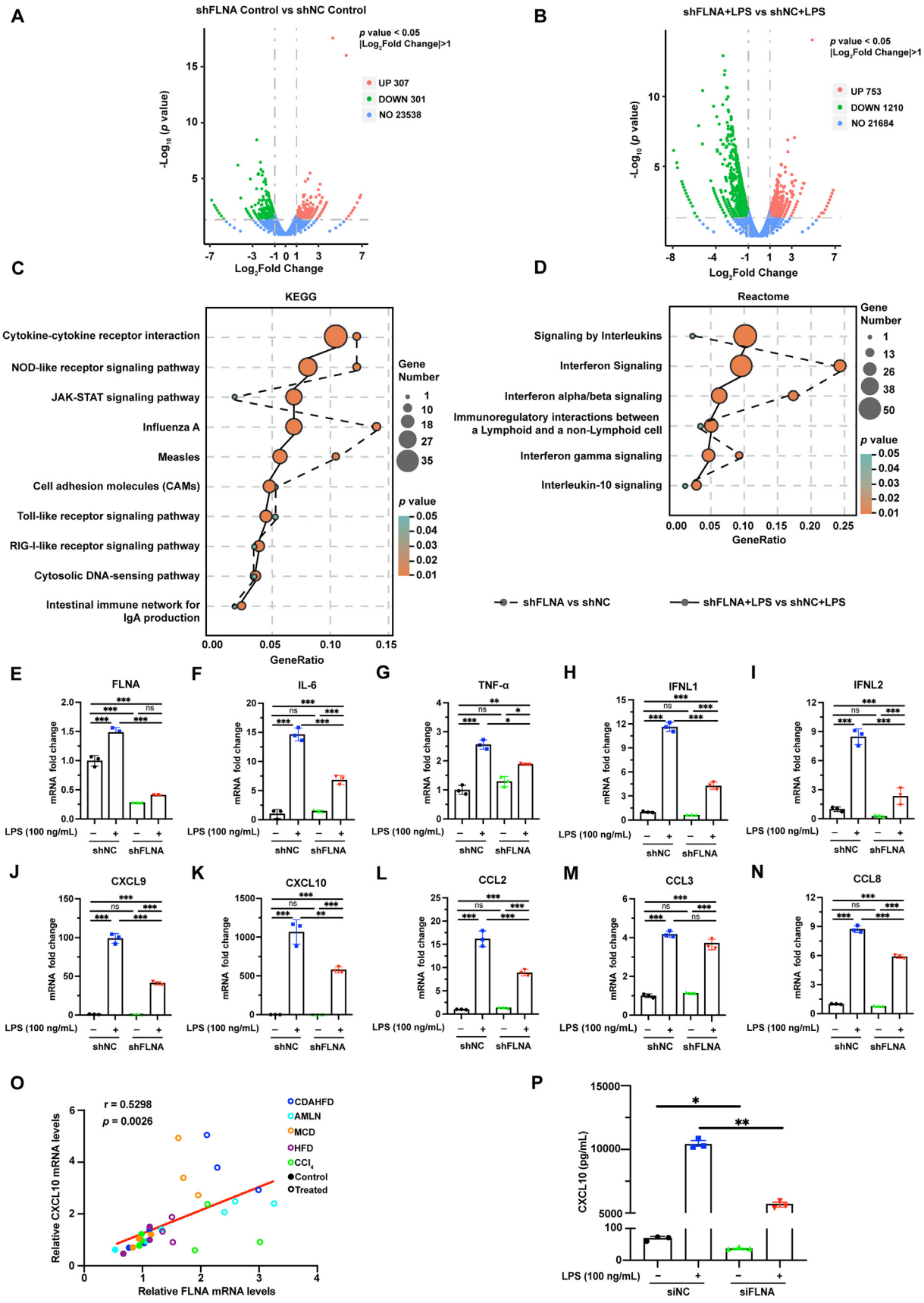

Fig. 2. Bioinformatic analysis and inflammatory factor expression levels in macrophages with FLNA knockdown. Volcano plots of gene expression changes in (A) shFLNA Control vs. shNC Control groups, and (B) shFLNA + LPS vs. shNC + LPS groups in PMA-derived THP-1 macrophages by quantitative transcriptome analysis. Red dots indicate upregulated DEGs, green dots indicate downregulated DEGs, and blue dots represent non-DEGs. (C) KEGG analysis of the downregulated DEGs. (D) Reactome analysis of the downregulated DEGs. mRNA levels of (E) FLNA, (F–I) cytokines (IL-6, TNF-α, IFNL1, IFNL2), and (J–N) chemokine ligands (CXCL9, CXCL10 CCL2, CCL3, CCL8). (O) Correlation analysis of CXCL10 and FLNA at mRNA level from the livers of mice steatohepatitis and fibrosis. (P) CXCL10 expression in RAW264.7 macrophages detected by ELISA with siRNA knockdown of FLNA and LPS stimulation. Data are mean ± SEM; $n = 3$. Ns: not significant, $^{*}p < 0.05$, $^{**}p < 0.01$, $^{***}p < 0.001$. (For interpretation of the references to colour in this figure legend, the reader is referred to the Web version of this article.)

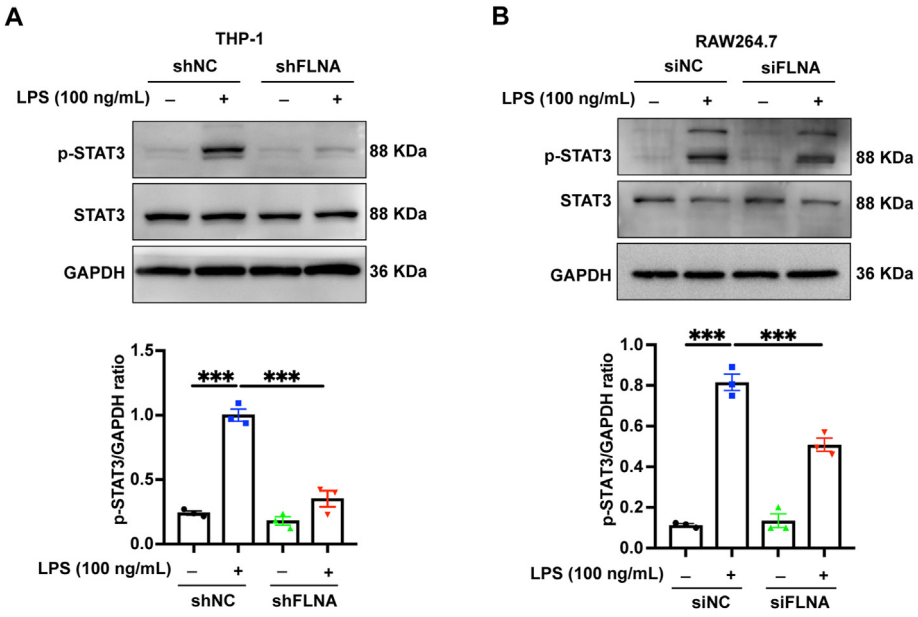

Fig. 3. FLNA knockdown inhibited LPS-induced STAT3 phosphorylation in macrophages. (A) The phosphorylation levels of STAT3 (Y705) in PMA-derived THP-1 cells with FLNA knockdown or LPS stimulation. (B) The phosphorylation levels of STAT3 (Y705) in RAW264.7 macrophages with FLNA knockdown or LPS stimulation. Data are mean ± SEM; $n = 3$. ***$p < 0.001$.

(Fig. 4B–C), and this increase was correlated with activation marker α-SMA (Fig. 4D). Then, lentivirus-mediated shRNA was used to knock down FLNA of LX-2 cells (Fig. 4E). Results showed that LPS-induced expression of TGF-β1 and CCL2 was reduced by FLNA knockdown (Fig. 4F–G). On the other hand, knockdown of FLNA increased the expression of pro-apoptotic proteins Caspase-7 and BAX (Fig. 4H–I) and reduced the expression of enzyme P4HA3 involved in collagen synthesis (Fig. 4J), while also upregulating matrix metalloproteinases (MMPs) MMP-1 and MMP-2 (Fig. 4K-L). These results suggested that FLNA may contribute to the fibrogenic function of HSCs.

4. Discussion

To date, increasing studies have focused on the mechanisms of NASH pathogenesis. Here, we aimed to understand the role of FLNA in the development of NASH. This study found that the mRNA and protein levels of FLNA were increased in the mice models of NAFLD/NASH and fibrosis (Fig. 1). The abnormal expression was associated with macrophages and HSCs (Fig. 1G–H), which are the primary cell sources that promote inflammation and fibrogenesis in NASH.

Liver macrophages, which include tissue-resident Kupffer cells and monocyte-derived macrophages, are important for maintaining liver homeostasis and immune regulation. In the condition of liver injury, the number of hepatic macrophages can increase significantly due to the influx of monocytes responding to chemokine signals such as CCL1/CCR8, CCL2/CCR2, and CXCL10/CXCR3 [16]. Previous studies have shown that FLNA is necessary for the migration and proliferation of monocyte in the conditions such as osteoclastogenesis and atherosclerosis [10,17]. This study found that FLNA was present in aggregated liver macrophages in NASH and regulated chemokines in macrophages, suggesting its role in promoting monocyte infiltration and expanding the hepatic macrophage population in NASH.

FLNA has been shown to interact with Toll-like receptor 4 (TLR4) and facilitate the release of inflammatory cytokines in Alzheimer's disease [18]. TLR4, which is found on the surface of various liver cells including hepatocytes, macrophages, and HSCs, has been linked to the progression of NASH [19–21]. LPS derived from gut bacteria is a major ligand of TLR4. Activation of TLR4 on the surface of liver cells by LPS can initiate an immune response that leads to the release of cytokines and immune mediators, causing liver inflammation and damage. Research has indicated that elevated levels of LPS in the bloodstream are linked to a heightened risk of developing NAFLD/NASH [22]. Based on these evidences, we speculate that FLNA participated in the LPS-TLR4 axis in the pathogenesis of NASH. Next, the role of FLNA in LPS-stimulated macrophages was examined. We found that FLNA knockdown in macrophages affected the expression of genes related to immune stress and inflammatory response, leading to decreased mRNA levels of inflammatory cytokines (IL-6, TNF-α, IFNL1, IFNL2) and chemokines (CCL2, CCL3, CCL8, CXCL9, CXCL10) and inactivation of STAT3 signaling pathway (Figs. 2 and 3). Inflammatory factors such as IL-6, TNF-α, CCL2, CCL3, CCL8, CXCL9, and CXCL10 have been implicated in the progression of NASH [23–27]. This study also showed a correlation between FLNA and CXCL10 (Fig. 2O), which is a key driver of inflammation in liver injury and steatohepatitis [26]. STAT3 is a cytoplasmic signaling transcription factor belonging to JAK-STAT pathways, which play an important role in mediating liver injury [28]. Previous research has proved that STAT3 could act as a downstream signal of TLR4 [29]. Taking together, we suggested that FLNA may connect TLR4 and STAT3 and promote the inflammatory response in NASH.

The HSCs are vital non-parenchymal cells in the liver. When the liver is damaged, HSCs can change from a quiescent to a profibrotic phenotype, contributing to the healing process through the secretion of ECM and proliferation. During the activation process, cytoskeletal reorganization plays an important role in the morphological and functional changes [30]. As the cytoskeletal actin-binding protein, FLNA has been related to cardiac fibroblast differentiation [12]. In this study, we observed an increase in FLNA mRNA expression during the activation of primary HSCs (Fig. 4B–D). When FLNA was knocked down, there was a decrease in the mRNA levels of TGF-β1 and CCL2 (Fig. 4F–G). TGF-β1 is a potent cytokine that stimulates HSC proliferation and differentiation, leading to the production of ECM [31]. CCL2, which is involved

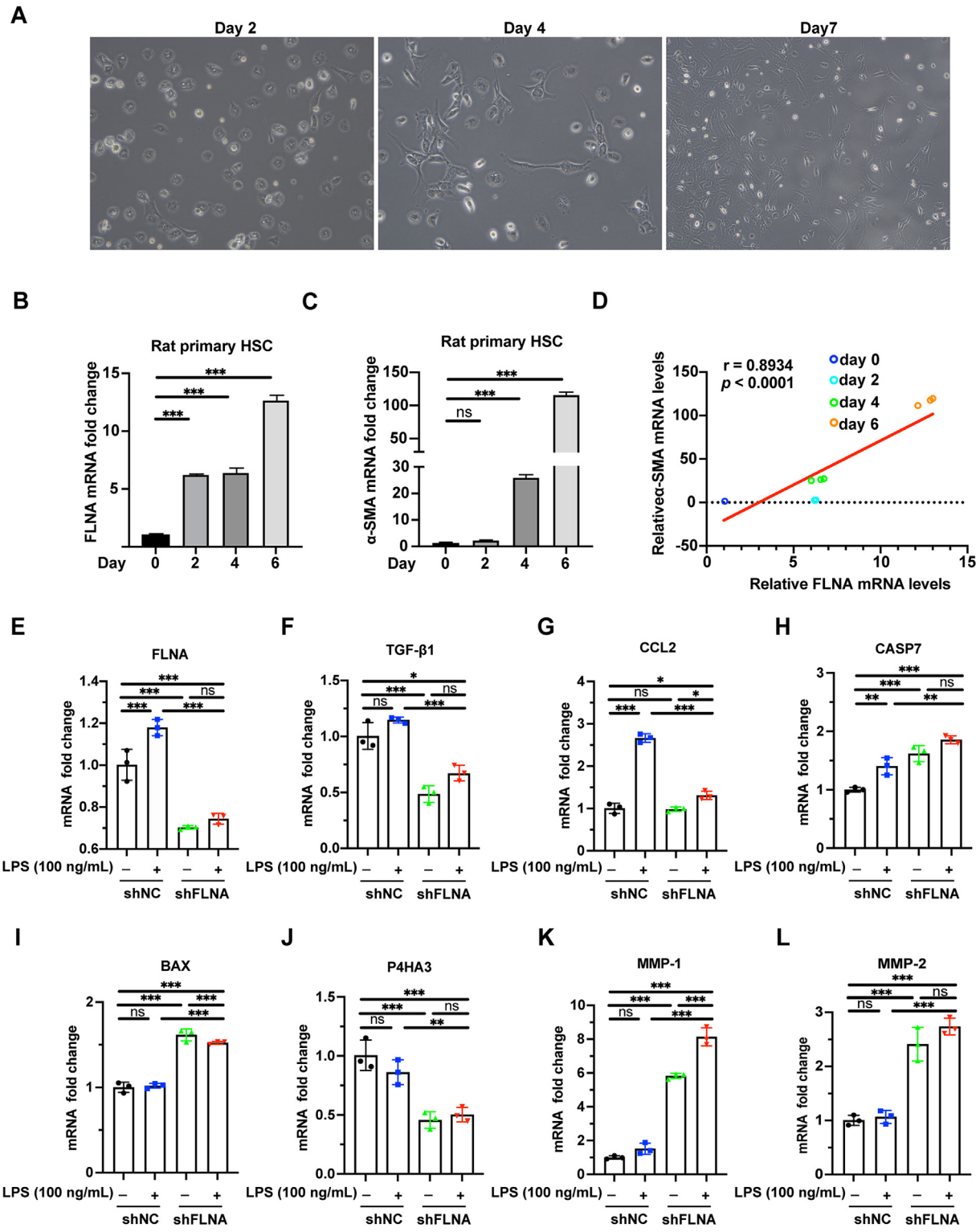

Fig. 4. FLNA in HSCs regulated the expression of cytokines, apoptosis proteins, and enzymes for ECM formation. (A) The morphology of primary rat HSCs from oval to star-like was recorded under a microscope at the indicated time points. The mRNA levels of (B) FLNA and (C) α-SMA during the activation of primary rat HSCs detected by qRT-PCR. (D) Correlation analysis of FLNA and α-SMA mRNA expression in primary rat HSCs. qRT-PCR analysis of LPS-induced mRNA expressions of (E) FLNA, (F–G) cytokines (TGF-β1, CCL2), (H–I) pro-apoptosis proteins (Caspase-7, BAX), (J) P4HA3 enzyme and (K–L) MMPs (MMP-1, MMP-2) in control or FLNA knockdown LX-2 cells. Data are mean ± SEM; $n = 3$. Ns: not significant, $^{*}p < 0.05$, $^{**}p < 0.01$, $^{***}p < 0.001$.

in liver inflammation and fibrosis [32], is induced in HSCs through various mechanisms including TGF-β1 and TLR4-mediated pathways [33,34]. These results suggested that FLNA may contribute to HSC activation and the production of profibrotic factors.

FLNA has also been linked to the remodeling of the pericellular collagen matrix. In NIH-3T3 fibroblasts, FLNA knockdown led to significant collagen degradation with upregulated MMP-9 but didn't have an effect on collagen mRNA [11]. Similar results were observed when FLNA was knocked down in HSCs, with an upregulation of the enzymes MMP-1 and MMP-2 (Fig. 4K-L). MMP-1 is responsible for the degradation of type I collagen in fibrotic liver. MMP-2 suppressed type I collagen expression and its deficiency exacerbated liver fibrosis in multiple mouse models [35]. These results suggest that FLNA may associate with ECM deposition in liver fibrosis. However, further research is needed to fully understand its role in the development of NASH and fibrosis in vivo.

In summary, we showed that FLNA expression was increased in the livers of mice with NAFLD/NASH and cirrhotic patients. The expression of the inflammatory and fibrotic mediators was reduced by FLNA knockdown in vitro. Partially, FLNA mediated downstream inflammatory cytokine release by promoting the phosphorylation of STAT3 Tyr705. Overall, FLNA may be a key factor in the progression of NASH.

Funding

This work was supported by the Science & Technology Department of Sichuan Province, China (No. 23NSFSC4173), the National Natural Science Foundation of China (NO. 81773375), and the “Zero to One” Innovation Research Project of Sichuan University (No. 2022SCUH0027).

Declaration of competing interest

The authors declare that there is no conflict of interest.

Acknowledgments

The authors thank the research platform provided by Food Safety Monitoring and Risk Assessment Key Laboratory of Sichuan Province.

Appendix A. Supplementary data

Supplementary data to this article can be found online at https://doi.org/10.1016/j.bbrc.2023.02.048.

References

[1] Z.M. Younossi, A.B. Koenig, D. Abdelatif, Y. Fazel, L. Henry, M. Wymer, Global epidemiology of nonalcoholic fatty liver disease-Meta-analytic assessment of prevalence, incidence, and outcomes, Hepatology 64 (2016) 73–84, https://doi.org/10.1002/hep.28431.

[2] N. Chalasani, Z. Younossi, J.E. Lavine, M. Charlton, K. Cusi, M. Rinella, S.A. Harrison, E.M. Brunt, A.J. Sanyal, The diagnosis and management of nonalcoholic fatty liver disease: practice guidance from the American Association for the Study of Liver Diseases, Hepatology 67 (2018) 328–357, https://doi.org/10.1002/hep.29367.

[3] J. Cai, X.J. Zhang, H. Li, The role of innate immune cells in nonalcoholic steatohepatitis, Hepatology 70 (2019) 1026–1037, https://doi.org/10.1002/hep.30506.

[4] O. Krenkel, F. Tacke, Liver macrophages in tissue homeostasis and disease, Nat. Rev. Immunol. 17 (2017) 306–321, https://doi.org/10.1038/nri.2017.11.

[5] K. Kazankov, S.M.D. Jorgensen, K.L. Thomsen, H.J. Moller, H. Vilstrup, J. George, D. Schuppan, H. Gronbaek, The role of macrophages in nonalcoholic fatty liver disease and nonalcoholic steatohepatitis, Nat. Rev. Gastroenterol. Hepatol. 16 (2019) 145–159, https://doi.org/10.1038/s41575-018-0082-x.

[6] A.X. Zhou, J.H. Hartwig, L.M. Akyurek, Filamins in cell signaling, transcription and organ development, Trends Cell Biol. 20 (2010) 113–123, https://doi.org/10.1016/j.tcb.2009.12.001.

[7] J. Zhou, X. Kang, H. An, Y. Lv, X. Liu, The function and pathogenic mechanism of filamin A, Gene 784 (2021), 145575, https://doi.org/10.1016/j.gene.2021.145575.

[8] T. Savinko, C. Guenther, L.M. Uotila, M. Llort Asens, S. Yao, S. Tojkander, S.C. Fagerholm, Filamin A is required for optimal T cell integrin-mediated force transmission, flow adhesion, and T cell trafficking, J. Immunol. 200 (2018) 3109–3116, https://doi.org/10.4049/jimmunol.1700913.

[9] H. Roth, M. Samereier, D. Begandt, R. Pick, M. Salvermoser, D. Brechtefeld, M. Schleicher, B. Walzog, A. Müller-Taubenberger, Filamin A promotes efficient migration and phagocytosis of neutrophil-like HL-60 cells, Eur. J. Cell Biol. 96 (2017) 553–566, https://doi.org/10.1016/j.ejcb.2017.05.004.

[10] S. Bandaru, C. Ala, R. Salimi, M.K. Akula, M. Ekstrand, S. Devarakonda, J. Karlsson, J. Van den Eynden, G. Bergstrom, E. Larsson, M. Levin, J. Boren, M.O. Bergo, L.M. Akyurek, Targeting filamin A reduces macrophage activity and atherosclerosis, Circulation 140 (2019) 67–79, https://doi.org/10.1161/CIRCULATIONAHA.119.039697.

[11] M. Mezawa, V.I. Pinto, M.P. Kazembe, W.S. Lee, C.A. McCulloch, Filamin A regulates the organization and remodeling of the pericellular collagen matrix, Faseb. J. 30 (2016) 3613–3627, https://doi.org/10.1096/fj.201600354RR.

[12] X. Li, M. Sun, S. Men, Y. Shi, L. Ma, Y. An, Y. Gao, H. Jin, W. Liu, Z. Du, The inflammatory transcription factor C/EBPbeta plays a critical role in cardiac fibroblast differentiation and a rat model of cardiac fibrosis induced by autoimmune myocarditis, Int. Heart J. 59 (2018) 1389–1397, https://doi.org/10.1536/ihj.17-446.

[13] D.E. Kleiner, E.M. Brunt, M. Van Natta, C. Behling, M.J. Contos, O.W. Cummings, L.D. Ferrell, Y.C. Liu, M.S. Torbenson, A. Unalp-Arida, M. Yeh, A.J. McCullough, A.J. Sanyal, Design and validation of a histological scoring system for nonalcoholic fatty liver disease, Hepatology 41 (2005) 1313–1321, https://doi.org/10.1002/hep.20701.

[14] Y. Liu, J. Brymora, H. Zhang, B. Smith, M. Ramezani-Moghadam, J. George, J. Wang, Leptin and acetaldehyde synergistically promotes αSMA expression in hepatic stellate cells by an interleukin 6-dependent mechanism, Alcohol Clin. Exp. Res. 35 (2011) 921–928, https://doi.org/10.1111/j.1530-0277.2010.01422.x.

[15] Y. Lu, X. Su, M. Zhao, Q. Zhang, C. Liu, Q. Lai, S. Wu, A. Fang, J. Yang, X. Chen, Y. Yao, Comparative RNA-sequencing profiled the differential gene expression of liver in response to acetyl-CoA carboxylase inhibitor GS-0976 in a mouse model of NASH, PeerJ 7 (2019), e8115, https://doi.org/10.7717/peerj.8115.

[16] J.Y. Cha, D.H. Kim, K.H. Chun, The role of hepatic macrophages in nonalcoholic fatty liver disease and nonalcoholic steatohepatitis, Lab Anim Res 34 (2018) 133–139, https://doi.org/10.5625/lar.2018.34.4.133.

[17] R. Leung, Y. Wang, K. Cuddy, C. Sun, J. Magalhaes, M. Grynpas, M. Glogauer, Filamin A regulates monocyte migration through Rho small GTPases during osteoclastogenesis, J. Bone Miner. Res. 25 (2010) 1077–1091, https://doi.org/10.1359/jbmr.091114.

[18] L.H. Burns, H.-Y. Wang, Altered filamin A enables amyloid beta-induced tau hyperphosphorylation and neuroinflammation in Alzheimer's disease, Neuroimmunol. Neuroinflammation 4 (2017), https://doi.org/10.20517/2347-8659.2017.50.

[19] J. Yu, C. Zhu, X. Wang, K. Kim, A. Bartolome, P. Dongiovanni, K.P. Yates, L. Valenti, M. Carrer, T. Sadowski, L. Qiang, I. Tabas, J.E. Lavine, U.B. Pajvani, Hepatocyte TLR4 triggers inter-hepatocyte Jagged1/Notch signaling to determine NASH-induced fibrosis, Sci. Transl. Med. 13 (2021), https://doi.org/10.1126/scitranslmed.abe1692.

[20] S.Y. Kim, J.M. Jeong, S.J. Kim, W. Seo, M.H. Kim, W.M. Choi, W. Yoo, J.H. Lee, Y.R. Shim, H.S. Yi, Y.S. Lee, H.S. Eun, B.S. Lee, K. Chun, S.J. Kang, S.C. Kim, B. Gao, G. Kunos, H.M. Kim, W.I. Jeong, Pro-inflammatory hepatic macrophages generate ROS through NADPH oxidase 2 via endocytosis of monomeric TLR4-MD2 complex, Nat. Commun. 8 (2017) 2247, https://doi.org/10.1038/s41467-017-02325-2.

[21] Z. Dong, Q. Zhuang, M. Ning, S. Wu, L. Lu, X. Wan, Palmitic acid stimulates NLRP3 inflammasome activation through TLR4-NF-κB signal pathway in hepatic stellate cells, Ann. Transl. Med. 8 (2020) 168, https://doi.org/10.21037/atm.2020.02.21.

[22] M.A. Hegazy, S.M. Mogawer, A. Alnaggar, O.A. Ghoniem, R.M. Abdel Samie, Serum LPS and CD163 biomarkers confirming the role of gut dysbiosis in overweight patients with NASH, Diabetes Metab Syndr Obes 13 (2020) 3861–3872, https://doi.org/10.2147/DMSO.S249949.

[23] X. Hou, S. Yin, R. Ren, S. Liu, L. Yong, Y. Liu, Y. Li, M.H. Zheng, G. Kunos, B. Gao, H. Wang, Myeloid-cell-specific IL-6 signaling promotes MicroRNA-223-enriched exosome production to attenuate NAFLD-associated fibrosis, Hepatology 74 (2021) 116–132, https://doi.org/10.1002/hep.31658.

[24] L. Xu, Y. Chen, M. Nagashimada, Y. Ni, F. Zhuge, G. Chen, H. Li, T. Pan, T. Yamashita, N. Mukaida, S. Kaneko, T. Ota, N. Nagata, CC chemokine ligand 3 deficiency ameliorates diet-induced steatohepatitis by regulating liver macrophage recruitment and M1/M2 status in mice, Metabolism 125 (2021), 154914, https://doi.org/10.1016/j.metabol.2021.154914.

[25] W. Wang, X. Liu, P. Wei, F. Ye, Y. Chen, L. Shi, X. Zhang, J. Li, S. Lin, X. Yang, SPP1 and CXCL9 promote non-alcoholic steatohepatitis progression based on Bioinformatics analysis and experimental studies, Front Med (Lausanne) 9 (2022), 862278, https://doi.org/10.3389/fmed.2022.862278.

[26] X. Zhang, J. Shen, K. Man, E.S. Chu, T.O. Yau, J.C. Sung, M.Y. Go, J. Deng, L. Lu, V.W. Wong, J.J. Sung, G. Farrell, J. Yu, CXCL10 plays a key role as an inflammatory mediator and a non-invasive biomarker of non-alcoholic steatohepatitis, J. Hepatol. 61 (2014) 1365–1375, https://doi.org/10.1016/

j.jhep.2014.07.006.
[27] C. Baeck, A. Wehr, K.R. Karlmark, F. Heymann, M. Vucur, N. Gassler, S. Huss, S. Klussmann, D. Eulberg, T. Luedde, C. Trautwein, F. Tacke, Pharmacological inhibition of the chemokine CCL2 (MCP-1) diminishes liver macrophage infiltration and steatohepatitis in chronic hepatic injury, Gut 61 (2012) 416–426, https://doi.org/10.1136/gutjnl-2011-300304.
[28] J. Zhao, Y.F. Qi, Y.R. Yu, STAT3: a key regulator in liver fibrosis, Ann. Hepatol. 21 (2021), 100224, https://doi.org/10.1016/j.aohep.2020.06.010.
[29] A. Rokan, J.C. Hernandez, R. Nitiyanandan, Z.Y. Lin, C.L. Chen, T. Machida, M. Li, J. Khanuja, M.L. Chen, S.M. Tahara, I. Siddiqi, K. Machida, Gut-derived endotoxin-TLR4 signaling drives MYC-ig translocation to promote lympho-proliferation through c-JUN and STAT3 activation, Mol. Cancer Res. 21 (2023) 155–169, https://doi.org/10.1158/1541-7786.Mcr-19-1209.
[30] X. Cui, X. Zhang, Q. Yin, A. Meng, S. Su, X. Jing, H. Li, X. Guan, X. Li, S. Liu, M. Cheng, F-actin cytoskeleton reorganization is associated with hepatic stellate cell activation, Mol. Med. Rep. 9 (2014) 1641–1647, https://doi.org/10.3892/mmr.2014.2036.
[31] F. Xu, C. Liu, D. Zhou, L. Zhang, TGF-beta/SMAD pathway and its regulation in hepatic fibrosis, J. Histochem. Cytochem. 64 (2016) 157–167, https://doi.org/10.1369/0022155415627681.
[32] S. Flamini, P. Sergeev, Z. Viana de Barros, T. Mello, M. Biagioli, M. Paglialunga, C. Fiorucci, T. Prikazchikova, S. Pagano, A. Gagliardi, C. Riccardi, T. Zatsepin, G. Migliorati, O. Bereshchenko, S. Bruscoli, Glucocorticoid-induced leucine zipper regulates liver fibrosis by suppressing CCL2-mediated leukocyte recruitment, Cell Death Dis. 12 (2021) 421, https://doi.org/10.1038/s41419-021-03704-w.
[33] S. Xi, X. Zheng, X. Li, Y. Jiang, Y. Wu, J. Gong, Y. Jie, Z. Li, J. Cao, L. Sha, M. Zhang, Y. Chong, Activated hepatic stellate cells induce infiltration and formation of CD163(+) macrophages via CCL2/CCR2 pathway, Front Med (Lausanne) 8 (2021), 627927, https://doi.org/10.3389/fmed.2021.627927.
[34] Y.H. Paik, R.F. Schwabe, R. Bataller, M.P. Russo, C. Jobin, D.A. Brenner, Toll-like receptor 4 mediates inflammatory signaling by bacterial lipopolysaccharide in human hepatic stellate cells, Hepatology 37 (2003) 1043–1055, https://doi.org/10.1053/jhep.2003.50182.
[35] M. Giannandrea, W.C. Parks, Diverse functions of matrix metalloproteinases during fibrosis, Dis Model Mech 7 (2014) 193–203, https://doi.org/10.1242/dmm.012062.